



## AN INNOVATIVE APPROACH TO MONITORING THE ACOUSTIC STATUS OF AN ENTIRE ROAD NETWORK

L. Schade<sup>1\*</sup>      A. Attenberger<sup>2</sup>      W. Bartolomaeus<sup>3</sup>  
 J. Gebhardt<sup>1</sup>      A. Hinträger<sup>2</sup>

<sup>1</sup> German Environment Agency (UBA), Dessau-Roßlau, Germany

<sup>2</sup> Bavarian Environment Agency (LfU), Augsburg, Germany

<sup>3</sup> Federal Highway Research Institute (BASt), Bergisch Gladbach, Germany

### ABSTRACT

Monitoring the acoustic status of an entire road network is hardly possible with available measurement systems at reasonable cost. While SPB measurements can be considered the gold standard and could be automated for long term monitoring, they provide information only for a specific observation site. CPX measurements are less accurate but allow for the assessment of road segments and in principle even entire road networks, alas at considerable cost and only for a snapshot in time. Against this backdrop, we have investigated the potential of a big data approach with a swarm of cheap microphones placed inside the air-filled cavity of tyres on regular passenger cars. The so-called SIT measurements (Sound Inside Tyre) pose many challenges in terms of data acquisition hardware and signal processing to retrieve information about the acoustic status of the road. We here present the development process and first results obtained with a prototype of the measurement system. The system proved to be robust in operation and capable to reliably detect the acoustic performance of different road surface types.

**Keywords:** noise abatement, road surface, tyre, monitoring

### 1. INTRODUCTION

Road traffic noise is omnipresent, with around 75 % of Germans feeling annoyed by it, as a representative survey by the German Environment Agency (UBA) shows [1]. While noise from the drive train dominates at low speeds up to about 20 to 30 km/h, tyre-road noise is the main source of noise in passenger cars at higher speeds. The keys to quiet traffic are therefore quiet tyres and quiet roads as well as low speeds.

But how loud or quiet are our roads? The national and European regulations for calculating noise emissions from roads know different surface course types and the associated emission parameters. The reality, however, is much more complex: not all new roads are built properly with respect to their acoustic performance, roads age and change their acoustic properties in the process, and roads are repaired with sometimes serious consequences for their acoustics. Therefore, regular monitoring of the acoustic status of the road network would make sense in order to specifically detect and remedy acoustic deterioration. Until now, such a comprehensive and regular monitoring has failed due to the lack of a suitable measurement method that would make such a monitoring cost-effective.

Currently, there are two standards for measuring the acoustic performance of a road, namely SPB measurements according to ISO 11819-1 [2] and CPX measurements according to ISO 11819-2 [3]. Both measurements require expensive equipment and skilled personnel and are therefore not well suited for monitoring entire road networks. The new measurement approach presented here aims to fill this gap.

\*Corresponding author: [lars.schade@umweltbundesamt.de](mailto:lars.schade@umweltbundesamt.de).

Copyright: ©2023 Schade et al. This is an open-access article distributed under the terms of the Creative Commons Attribution 3.0 Unported License, which permits unrestricted use, distribution, and reproduction in any medium, provided the original author and source are credited.

## 2. CONCEPTUAL FRAMEWORK

To enable network-wide monitoring, the new method had to have two key characteristics: First, the hardware must be robust and inexpensive, and second, the system must be easy for laypeople to operate. A swarm of these devices could then collect data continuously and upload it to a central server. Even if the quality of the individual measurements is not particularly high, a statistical analysis of the entire data set would allow reliable conclusions to be drawn about the acoustic status of the road network.

To meet the requirement for robustness, we decided to place the microphone inside the tyre cavity. We therefore refer to the approach as Sound Inside Tyre (SIT) measurement. This idea goes back to the work of Oskar Bschorr in the early 1980s [4] when he was the first to study the sound inside a tyre.

The two main challenges we faced were developing the necessary hardware and researching how best to extract information from the SIT signal. The following two sections deal with each challenge separately.

## 3. HARDWARE

The SIT measurement system consists of two main parts, the wheel unit and the on-board unit. The wheel unit is comprised of the microphone mounted to the rim and the microphone electronics mounted to the outside of the rim, both connected via a cable. When designing the wheel unit, it was important that there should be no structural interference with the wheel. To fit into the standard valve bore of steel rims, a component was developed that has a

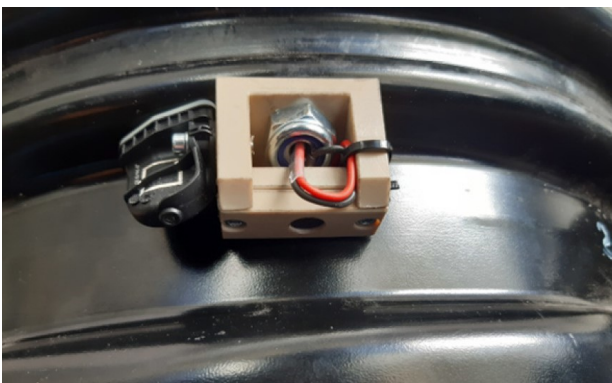


**Figure 1.** Microphone holder (beige) with a tyre pressure monitoring system (TPMS) attached to the left.

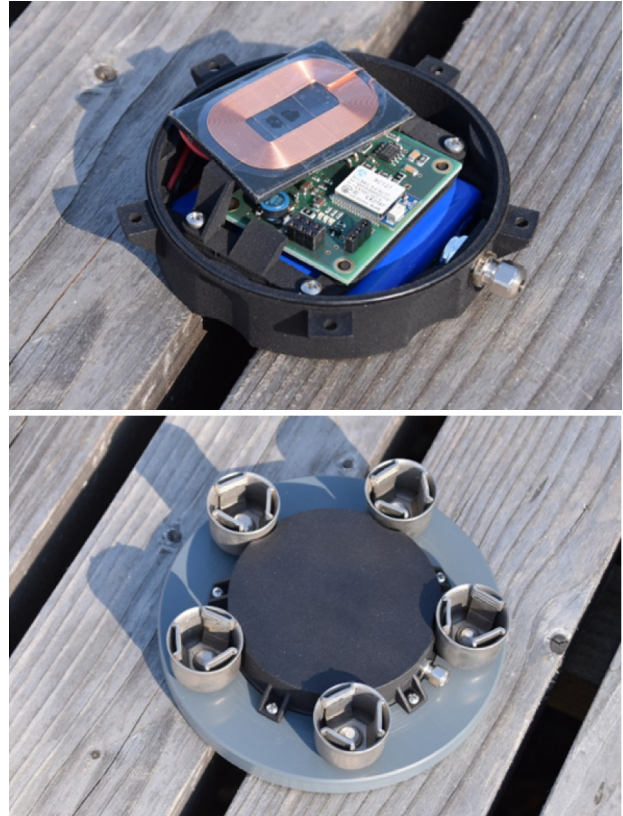


**Figure 2.** Container for the microphone electronics: Open container (top) and closed container with the clamps for the wheel bolts (bottom).

microphone holder on the inside of the rim, provides pressure-tight routing of the signal cable and allows normal tyre inflation (Fig. 1). Different microphones were tested for their suitability for SIT measurements. A high-quality piezoelectric microphone with acceleration compensation served as a reference, but is unsuitable for fleet use due to its price of around 3,000 euros. Among the microphones examined, a simple electret condenser microphone proved to be sufficiently accurate for our application, at a unit price of only about one euro [5]. The electronics for amplifying the microphone signal and transmitting the signal to the on-board unit have been miniaturised so that they fit in a small container within the circle of the wheel bolts. This container is clamped directly onto the wheel bolts and powered by a rechargeable battery that can be charged inductively, so the wheel unit is completely sealed against water and dirt (Fig. 2).

The on-board unit is responsible for processing and storing the data and also enriching the data stream with GPS information. It consists of a Raspberry Pi and is powered by the vehicle's on-board voltage. It communicates with the wheel unit via Bluetooth and can automatically upload data to a central cloud server via Wifi when the vehicle is parked within range of its Wifi home network.

#### 4. THE SIT SIGNAL

At first glance, the noise inside the tyre bears little resemblance to the noise at the roadside, which is what we are actually interested in. In fact, the fundamental question is why and to what extent it is possible at all to extrapolate from the noise inside the tyre to the noise at the roadside. The noise we refer to as tyre-road noise is generated by different mechanisms. Fundamentally, only those mechanisms associated with vibration excitation of the tyre can be reflected in the SIT signal.

##### 4.1 Main Characteristics of the SIT Signal

In the acoustically relevant frequency range up to 5 kHz, the SIT signal is characterised by the normal modes of the tyre and the normal modes of the torus-shaped volume of air enclosed inside the tyre. In the following, we simply refer to tyre modes and torus modes.

The tyre modes are excited by the flattening of the tyre in the contact patch with the road and are therefore synchronised with the rotation rate of the tyre. Their frequencies thus depend on the vehicle speed. Equation (1) defines the frequency of the  $n^{\text{th}}$  tyre mode  $f_{\text{tyre},n}$  as a function of the vehicle speed  $v$  and the radius of the wheel  $r_{\text{tyre}}$ :

$$f_{\text{tyre},n} = \frac{v}{2\pi \cdot r_{\text{tyre}}} \cdot n \quad (1)$$

The natural frequencies of the torus modes depend only on the geometric dimensions of the torus and are independent of the vehicle speed. According to Equation (2), the frequency of the  $n^{\text{th}}$  torus (longitudinal) mode  $f_{\text{torus},n}$  depends only on the effective radius of the torus  $r_{\text{torus}}$  and the speed of sound in air  $c_{\text{air}}$ :

$$f_{\text{torus},n} = \frac{c_{\text{air}}}{2\pi \cdot r_{\text{torus}}} \cdot n \quad (2)$$

For car tyres and a vehicle speed of 80 km/h, this gives a frequency of about 12 Hz for the first tyre mode and of about 220 Hz for the first torus mode.

A typical spectrum of the SIT signal with 1 Hz resolution is shown in Figure 3. The spectrum is Z-weighted. Tyre modes are visible by eye up to an order of about 90. The first four torus modes are also easily visible. The spectral peaks reach values up to 140 dB(Z) with an overall sound pressure level of 148 dB(Z).

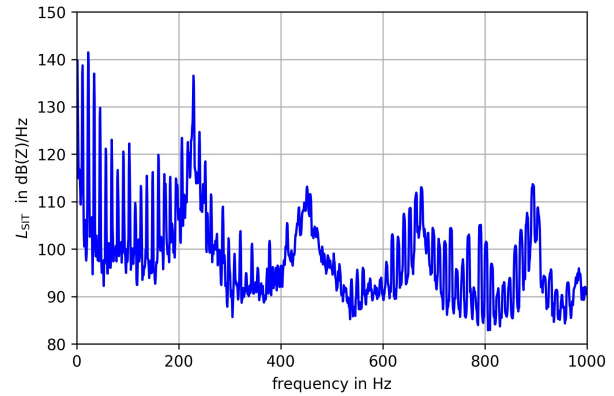


**Figure 3.** SIT spectrum of a car tyre at 80 km/h, Z-weighted with 1 Hz resolution.

To investigate which parameters the SIT signal depends on, tests were conducted in the controlled environment of the vehicle-pavement interaction facility (“Prüfstand Fahrzeug-Fahrbahn”, PFF) of the Federal Highway Research Institute (BAST) [6]. In these tests the test drum was equipped with a fine grained and smooth test surface, referred to as safety walk, and brought to a speed of 120 km/h. The drum was then let to spin-down freely to a speed of 30 km/h and SIT and CPX measurements were conducted simultaneously. In an additional set of tests both the tyre inflation pressure and the wheel load were varied to investigate the influence of these two parameters. And in a final test a spin-down was measured twice under identical conditions with the only difference that the tread pattern of the test tyre was shaved off in between the tests. Some key findings are shown in the Z-weighted spectrograms of Figure 4: The centre panel displays the SIT spectrogram of a car tyre; at low frequencies up to about 200 Hz the speed dependent tyre modes dominate while the torus modes dominate at higher frequencies. The simultaneously recorded CPX spectrogram is shown in the bottom panel; Tyre and torus modes are barely visible and – besides broad band noise at higher speeds and well below 100 Hz – the CPX spectrum is characterized by a broad maximum around 1 kHz. The top panel displays the SIT spectrum of the tyre after the tread pattern was completely shaved off; the resemblance to the centre panel is remarkable and underlines that the basic

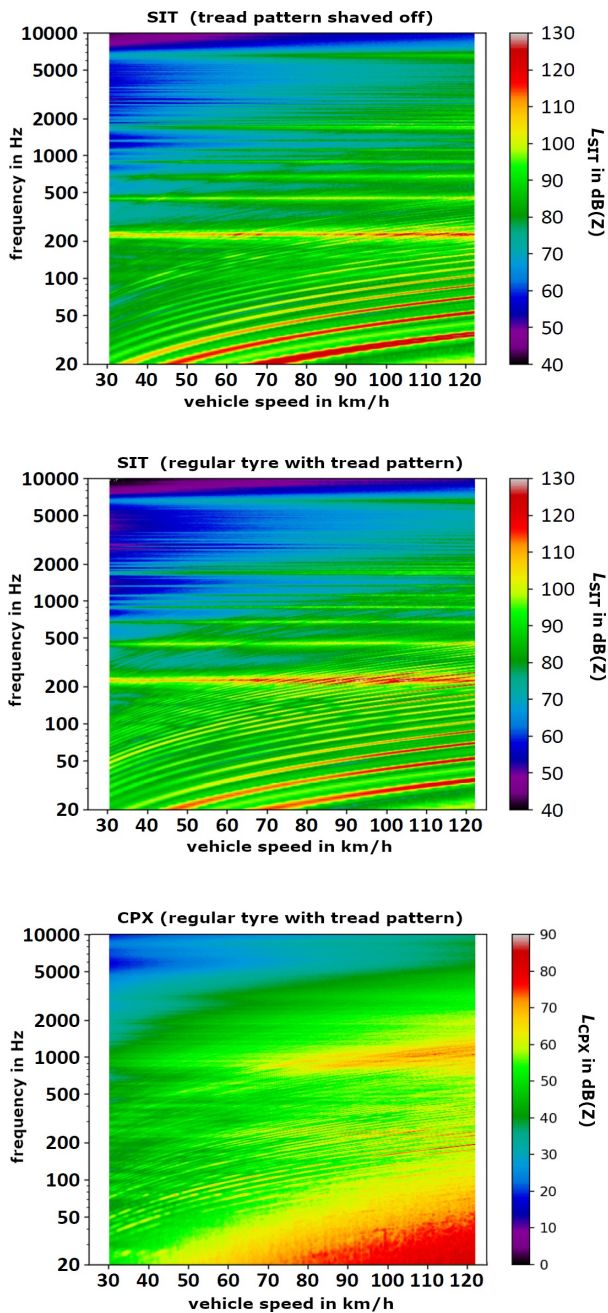
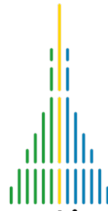


**Figure 4.** Spectrograms of tests at the vehicle-pavement interaction facility of the BAST: Shown is data from spin downs from an initial speed of 120 km/h down to 30 km/h. The SIT signal of a car tyre (centre), the simultaneously recorded CPX signal (bottom), and the SIT signal of the same tyre after shaving the tread pattern off (top).

characteristics of the spectrogram do not depend on the tread depth or even the existence of a tread pattern. Overall the tests at the vehicle-pavement interaction facility indicated that a big data set of SIT measurements should be useful even without knowledge of parameters such as tread depth, inflation pressure and wheel load.

#### 4.2 How to extract information from the SIT signal?

Initially we considered the tyre modes as unwanted signal and attempted to design a filter to free the SIT signal from the tyre modes. In field tests it turned out that in some cases even the 90<sup>th</sup> tyre mode could reliably be detected while in other cases only the first 35 tyre modes were detectable. And it turned out that there is a good correlation between the type of the road surface and the number of tyre modes detectable in the SIT signal (NDTM). This effect is illustrated in Figure 5 which compares the SIT spectrum of a SMA 8 (stone mastic asphalt with a maximum grain size of 8 mm) with that of a DSH-V 5 (thin layer asphalt built hot on sealing with maximum grain size of 5 mm). The DSH-V 5 surface is less noisy and allows for the detection of about 75 tyre modes in comparison to around 60 being detectable on the SMA 8 surface.

How well the parameter NDTM corresponds to the road surface type can be seen in Figure 6 which displays data from an almost 30 km long test drive on the German Federal Road B2 close to the city of Augsburg. The car was driven at 80 km/h. The road surface type changes several times along the road from DSH-V to SMA and back again.

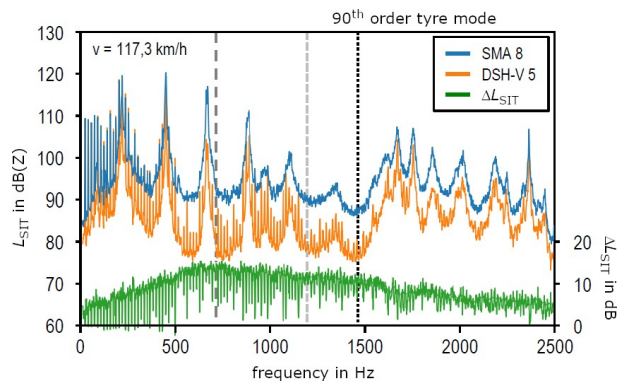


**Figure 5.** Comparison of SIT spectra from two different road surface types, namely SMA 8 (stone mastic asphalt with max. grain size of 8 mm) and DSH-V 5 (thin layer asphalt built hot on sealing with max. grain size of 5 mm).

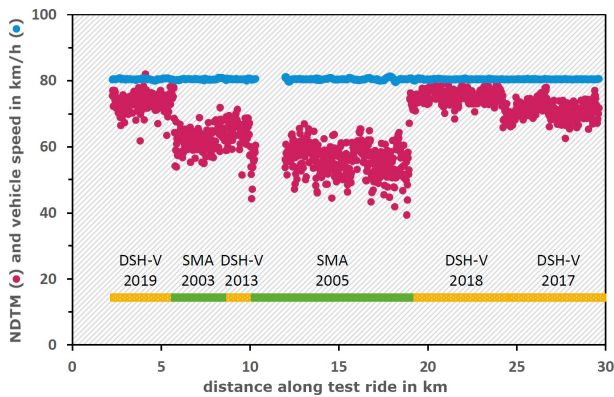


**Figure 6.** Data from a test drive along German Federal Road B2: Each point represents a section of 20 m length along the road. The red dots show the number of detectable tyre modes and the blue dots the vehicle speed in km/h. The bar in the lower part of the figure demarks the road surface type and the year of construction.

Also shown is the year of construction of the respective road section. It is clearly visible that each section has its own “finger print” in terms of NDTM. The well-known acoustic aging effect of DSH-V surfaces is also visible in the data. While the different road sections can easily be distinguished from one another, some of the sections feature a rather large variance in terms of NDTM.

An important advantage of using the parameter NDTM instead of the sound power level is the independence from absolute levels. Since it is impossible to calibrate the SIT microphone regularly, this advantage weighs heavily. The physical interpretation of the parameter NDTM is not obvious. We suggest that at frequencies above that corresponding to the highest detectable tyre mode the directly forced excitation by the road masks the tyre modes. This frequency can thus be interpreted as the masking wavelength  $\lambda_{\text{mask}}$  of the road surface and is calculated by use of the following equation:

$$\lambda_{\text{mask}} = \frac{2\pi \cdot r_{\text{tyre}}}{\text{NDTM}} \quad (3)$$

To limit the amount of data and in analogy to the CPX standard, the masking wavelength is calculated for road segments of 20 m length each. It should be noted that the detection of the masking wavelength fails if the vehicle is accelerating or breaking, i.e. if the tyre is under

considerable torque. Therefore, segments with an acceleration in excess of  $\pm 0.2 \text{ ms}^{-2}$  should be excluded from further analysis and be dropped.

#### 4.3 Mapping function between SIT data and SPB data

SPB measurements according to ISO 11819-1 are considered the gold standard for the assessment of the noise emissions of a road. Therefore, a key question is whether a mapping function can be derived to reliably infer equivalent SPB sound pressure levels from SIT data, specifically from the masking wavelength. To address this question six test locations on public roads close to Augsburg were chosen (Fig. 7). These locations are characterized by homogeneity in terms of the masking wavelength and feature three different dense road surface types, namely SMA, DSH-V and WB (exposed aggregate concrete). At each of these test sites, SPB measurements were conducted according to ISO 11819-1 and SIT measurements with four different test vehicles at speeds of 80, 100, and 120 km/h, respectively. The results of the SIT measurements are summarized in Figure 8. The different colours correspond to the different vehicles with black ( $t = 5$ ) denoting the SIT device on the CPX trailer. Three aspects of the measurements are clearly visible: The masking wavelength slightly depends on the vehicle speed with higher speeds corresponding to smaller

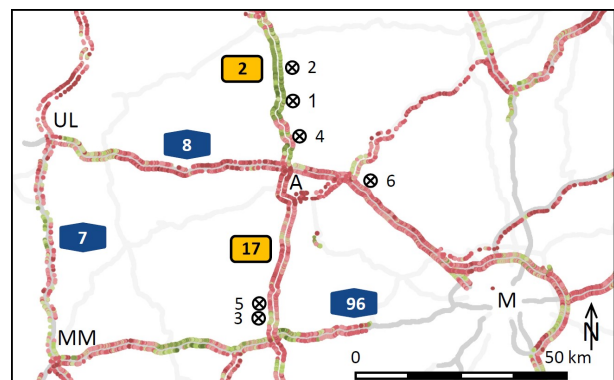


**Figure 7.** Map showing the six test locations around the city of Augsburg (A). The coloured dots represent results of SIT measurements with a colour scheme from green to red for the masking wavelength.

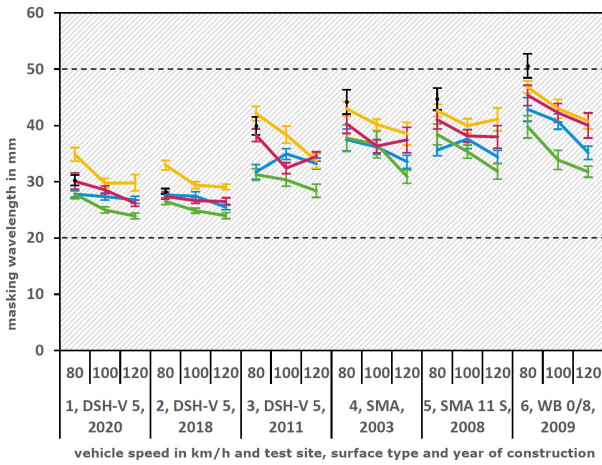


**Figure 8.** Summary of the results of the SIT measurements at the six test locations shown in Figure 7. Each colour corresponds to one of the SIT devices (i.e. test cars) used.

wavelengths, i.e. to higher values of NDTM. There is a considerable spread in the results obtained with the different SIT devices owing to the use of different tyres and different cars. This spread is small enough to allow for a reliable detection of the site-to-site differences in the masking wavelength.

Finally, the masking wavelengths can be compared to the maximum pass-by levels of the SPB measurements. In the top panel of Figure 9 the SPB levels are plotted against the average masking wavelengths of the SIT devices at the six test sites and separately for the three vehicle speeds used. For each vehicle speed a linear regression is calculated and the resulting offset and slope parameters are plotted against the vehicle speed in the bottom panel of Figure 9 featuring a linear relationship. An equivalent SPB level can thus be derived from the average masking wavelength with the following set of equations:

$$L_{\text{SIT,eq}} = a_v + b_v \cdot \lambda_{\text{mask}} \quad (4)$$

$$a_v = 74.5 \text{ dB(A)} - 0.27 \frac{\text{dB(A)} \cdot \text{s}}{\text{m}} \cdot v \quad (5)$$

$$b_v = 61.8 \frac{\text{dB(A)}}{\text{m}} + 12.7 \frac{\text{dB(A)} \cdot \text{s}}{\text{m}^2} \cdot v \quad (6)$$

With this approach to analysing the SIT signal, the principal feasibility of deducing equivalent SPB levels without the need for a calibration of the SIT devices has been accomplished.

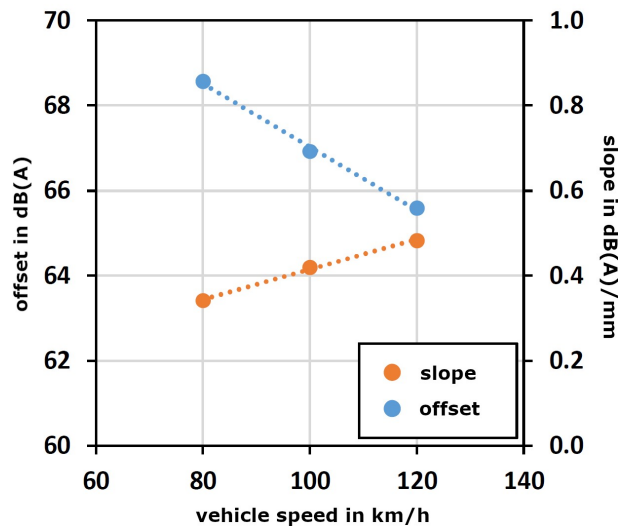
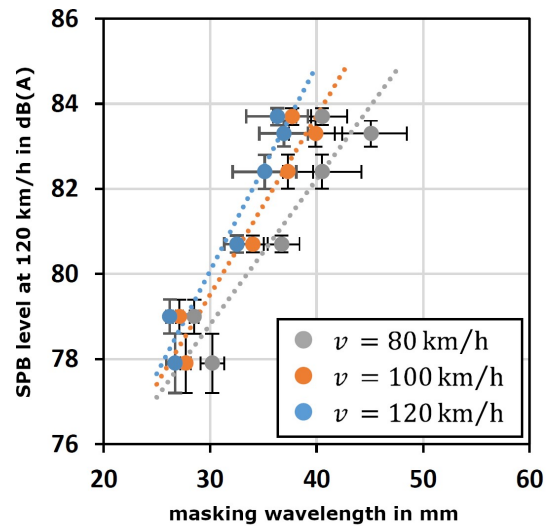


**Figure 9.** Comparison of the “ground truth” SPB levels to the masking wavelengths of the SIT measurements. Masking wavelengths (averages from the SIT devices) at the six locations for the three vehicle speeds used (top), and speed dependence of the regression parameters (bottom).

## 5. A FIRST PRACTICAL FLEET TEST

The logical next step was to test the system in the field with a small fleet experiment. Four vehicles of the car pool of the Bavarian Environment Agency (LfU) were equipped with SIT devices and Wifi hubs installed at the vehicles home base for regular automated data upload to a central cloud server. Various staff had access to the vehicles. An information sheet informed the drivers about the installed SIT devices and asked for a defensive driving style avoiding accelerations where possible. No further training was necessary as the SIT devices operated completely unsupervised. The only maintenance needed was recharging of the wheel units about once a month, triggered by an automatic low-voltage alarm of the SIT device and realized by instructed layman with an inductive charger, i.e. without need for tools.

Over a period of three years, a total road length of about 3850 km composed of about 192'500 road segments of

20 m length each were surveyed and acoustically analysed. The deduced equivalent SPB levels were compared to the theoretically predicted levels according to the German guidelines for noise protection on roads (“Richtlinien für den Lärmschutz an Straßen”, RLS-19). This difference between theory and observation is shown in Figure 10: Red dots denote segments which were observed to be noisier than predicted by theory, yellow dots denote somewhat quieter segments with a difference in the range of 0 to 3 dB, and green dots stand for the remaining segments which were found to be more than 3 dB quieter than predicted by the RLS-19. The surveyed road network proved to be largely in an acoustically good condition. Nevertheless, about 15 % of the network was found to be noisy with respect to the RLS-19 indicating a potential need for maintenance or resurfacing.

More details on the hardware development, the data analysis, and the fleet experiment can be found in [8].

## 6. OUTLOOK

The general feasibility and usefulness of the SIT approach has been demonstrated with the tests presented here. The potential to usefully complement the well-established SPB and CPX approaches is apparent. Yet a number of open questions and challenges remain. To name a few:

- How can the SIT approach be extended to heavy goods vehicles?
- How can the SIT approach be amended to operate on absorbing road surface types?
- How can the SIT approach be applied at lower speeds of 50 km/h and below?
- How can, in a scenario with a large fleet of SIT devices, the potential of big data be best exploited?
- How can the theoretical foundation of the SIT approach be advanced and used to optimize the system?

It remains to be seen, whether these questions can be answered in a satisfactory way and open the floor for a wider application of the SIT approach.

## 7. REFERENCES

- [1] BMUV/UBA (Eds.): *Umweltbewusstsein in Deutschland 2020*, Berlin, 2022.
- [2] ISO: *Acoustics — Measurement of the influence of road surfaces on traffic noise — Part 1: Statistical*

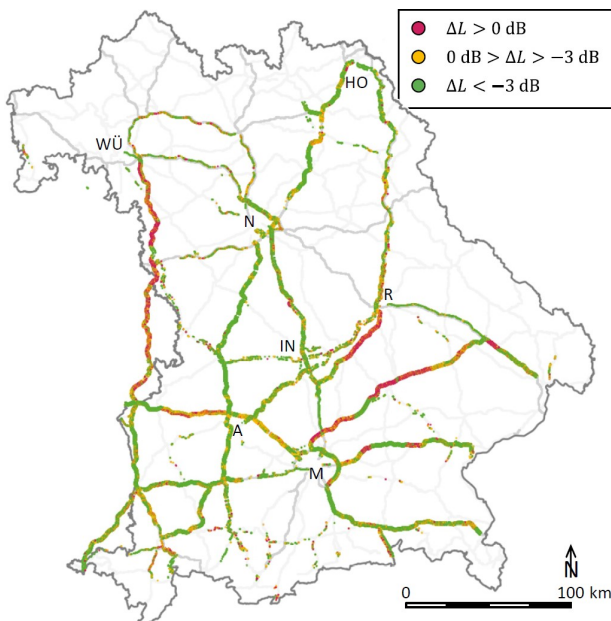


**Figure 10.** Map of Bavaria showing the results of the fleet experiment. Each coloured dot represents the rating of a 20 m road segment. The rating is based on the difference of the equivalent SPB level  $L_{SIT,eq}$  of Equation (4) and the noise level predicted by the German guidelines for noise protection on roads (“Richtlinien für den Lärmschutz an Straßen”, RLS-19) [7].

*pass-by method (ISO Standard No. 11819-1:2023), 2023.*

- [3] ISO: *Acoustics — Measurement of the influence of road surfaces on traffic noise — Part 2: The close-proximity method (ISO Standard No. 11819-2:2017), 2017.*
- [4] O. Bschorr and R. Kühne: “Bestimmung der akustischen Qualität von Straßen”, *Lärmbekämpfung*, pp. 144-148, 2007.
- [5] J. Masino, M. Frey and F. Gauterin: *Technische Aspekte der Überwachung der akustischen Qualität der Fahrwege im Straßenverkehr*. UBA-Texte 101/2018, 2018. ISSN 1862-4359.
- [6] W. Bartolomaeus: *Vehicle-pavement interaction facility (PFF)*. Federal Highway Research Institute, 28.04.2023: [https://www.bast.de/EN/Traffic\\_Engineering/Technology/PFF.html](https://www.bast.de/EN/Traffic_Engineering/Technology/PFF.html)
- [7] FGSV e. V. (Ed.): *Richtlinien für den Lärmschutz an Straßen – RLS-19*. FGSV e. V. Köln, 2019. ISBN 978-3-86446-256-6
- [8] A. Hinträger und A. Attenberger: *Überwachung der akustischen Qualität des Straßennetzes mittels Reifen-Torus-Messungen*. UBA-Texte 37/2023, 2023. ISSN 1862-4804